Available online at www.sciencedirect.com

SciVerse ScienceDirect

Journal of the European Ceramic Society 32 (2012) 937–945

www.elsevier.com/locate/jeurceramsoc

Interaction of molten aluminum with porous TiB_2-based ceramics containing Ti–Fe additives

Hamed Heidari [a], Houshang Alamdari [a,*], Dominique Dubé [a], Robert Schulz [b]

[a] *Department of Mining, Metallurgical and Materials Engineering, Université Laval, Québec, QC, Canada G1V 0A6*
[b] *Hydro-Quebec Research Institute, 1800 Boul. Lionel Boulet, Varennes, QC, Canada J3X 1S1*

Received 1 September 2011; received in revised form 21 October 2011; accepted 29 October 2011
Available online 21 November 2011

Abstract

In this study, the wettability and interaction of porous TiB_2-based composites with liquid aluminum has been investigated. TiB_2 composites were consolidated with Ti and Fe additives using pressureless sintering. The composites show good wettability with respect to molten aluminum. During liquid infiltration, Ti and Fe additives are dissolved. Intermetallic compounds containing Ti, Fe and Al are formed within the penetration depth. Since these phases have melting points higher than the experiment's temperature (960 °C), isothermal solidification takes place during the penetration of molten aluminum. Liquid aluminum does not seem to attack the solid skeleton of the TiB_2 specimens and no signs of swelling or cracking were detected.
© 2011 Elsevier Ltd. All rights reserved.

Keywords: Electron microscopy; Porosity; Microstructure-final; Borides; Wettable cathode

1. Introduction

Molten aluminum reacts with almost all materials except with some ceramics such as borides which exhibit very good stability in liquid Al.[1] Due to its intrinsic stability, high electrical conductivity and good wettability with respect to liquid aluminum, TiB_2 has been extensively investigated as an alternative for graphite cathodes in aluminum smelters. It has been mentioned that by replacing graphite cathodes by TiB_2 electrodes, more than 10% of the energy required to produce aluminum could be saved.[2–4]

However, the fabrication of large and dense TiB_2 parts is quite complicated[5,6] due to the poor sinterability of the material. Consolidation of pure TiB_2 requires very high temperatures. At temperatures higher than 1700 °C however, exaggerated grain growth occurs leading to materials with poor mechanical and thermal shock resistances.[7,8] In TiB_2 ceramics consolidated with current methods, liquid Al is able to penetrate the grain boundaries and this leads to cracking of components due to the low toughness of materials.[3,9,10] Micro-cracks can result from the anisotropic thermal expansion of TiB_2 or from the formation of phases with higher molar volumes[11] when liquid Al reacts with grain boundary impurities.

The addition of sintering aids is a way to lower the consolidation temperature and hence prevent the exaggerated grain growth. The use of iron, chromium and nickel as sintering aids for TiB_2 has been reported.[12–14] In a previous work, 7 wt% Ti and 3 wt% Fe were added to TiB_2 particles to promote liquid phase sintering during consolidation.[15,16] Sintering of specimens at 1650 °C for 1 h resulted in a relative density of 91% and a bending strength of 300 MPa. No attempt was made to achieve higher densities because it was expected that the presence of uniformly distributed small porosities could help to prevent the propagation of micro-cracks when samples are in contact with molten aluminum. However, porosities ease melt penetration since liquid Al wets TiB_2 quite well.[17,18]

In this work, the reaction of porous TiB_2 composites containing 7 wt% Ti and 3 wt% Fe additives with molten aluminum was investigated. Microstructural characterizations were performed in order to understand the reaction mechanisms between the composites and liquid aluminum.

* Corresponding author at: Département de génie des mines, de la métallurgie et des matériaux, Pavillon Adrien-Pouliot 1065, av. de la Médecine, Québec (Québec), Canada G1V 0A6. Tel.: +1 418 656 2131x7666; fax: +1 418 656 5343.
E-mail address: houshang.alamdari@gmn.ulaval.ca (H. Alamdari).

0955-2219/$ – see front matter © 2011 Elsevier Ltd. All rights reserved.
doi:10.1016/j.jeurceramsoc.2011.10.053

2. Materials and methods

The TiB_2 composites were prepared by mixing commercially pure TiB_2 powder (2–10 μm) with 10 wt% of pre-alloyed additives in powder form (7 wt%Ti and 3 wt%Fe). The additives (a mixture of Ti and FeTi phases) were then milled with TiB_2 for 30 min using a high-energy ball mill. The powder was compacted with a uniaxial pressure and sintered for 1 h at 1650 °C under an Ar–5%H_2 atmosphere.[15]

Sessile drop tests were used to investigate the wettability of the specimens with liquid aluminum. An Al pellet (0.09 g) was used for the experiments. The surface of the Al pellet was polished prior to the test in order to reduce surface oxides. The pellet was placed on top of the specimen in a resistance tube furnace under high vacuum (10^{-3} Pa). The furnace was heated up rapidly to 960 °C (corresponding to the operating temperature of aluminum electrolysis cells) and kept at this temperature. A light was fixed at one end of the tube and the image of the Al drop over the specimen was recorded at the other end during the experiment. A software was used to evaluate the contact angle between the specimen surface and the aluminum drop from the recorded images. The reported contact angle is the average of left and right side angles. The time $t = 0$ was set when the specimens' temperature reached 700 °C approximately and a spherical liquid Al drop formed over the surface of the sample. After the experiment, the furnace was cooled down at a rate of about 15 °C/min below the melting point of pure aluminum.

The surface of some TiB_2 samples was polished before the tests in order to remove surface contamination, especially oxides. Polishing was carried out using a diamond abrasive (6 μm) followed by cleaning with isopropanol in an ultrasonic bath. Therefore, experiments were performed on polished surfaces (identified as S1-P, P: Polished) as well as on as-sintered surfaces (identified as S2-AS, AS: As Sintered).

For one specimen, the sessile test was performed using a bigger Al pellet (0.18 g). In this case, the early stage of the liquid infiltration process was investigated by interrupting the experiment after $t = 100$ min. The sample was identified as S3-PP (PP: Partially Penetrated). In a last experiment, a polished specimen was subjected to a complete sessile drop test then, another aluminum piece was placed on the same surface and a second sessile drop experiment was conducted (S4-2D, 2D: 2nd Drop).

Reactions between liquid aluminum and ceramics were investigated by examining the cross-sections of the specimens. The samples were mounted in epoxy resin, cut using a diamond saw and polished down to 0.1 μm. The final polishing was performed using a 0.05 μm alumina suspension. The microstructure of specimens was investigated using a scanning electron microscope (SEM) equipped with an energy dispersive X-ray detector (EDX). Electron probe microanalysis (EPMA) was performed for elemental mapping of aluminum, titanium, iron and oxygen. Focused ion beam (FIB) was used to prepare samples for transmission electron microscopy (TEM) characterization. Phase identification was carried out based on selected area electron diffraction (SAED) pattern analysis.

3. Results and discussion

3.1. Sessile drop tests

Fig. 1 shows images of a molten aluminum drop on the surface of a polished specimen (S1-P) during a sessile drop test after different time intervals. The measured average contact angles (average between the right and left contact angle) is shown below each figure. During the experiment, the Al drop spreads over the surface and penetrates inside the specimen. After 9 min, the specimen temperature was about 870 °C and there was no visible wetting. After 22 min, the temperature reached 940 °C, wetting occurred and the contact angle was about 85 °. The measured contact angles after 30 and 50 min were 29 and 6 °, respectively.

Fig. 2 shows the average contact angle as a function of the elapsed time for the polished (S1-P) and the as-sintered specimen (S2-AS). Two steps can be distinguished in the case of the S2-AS sample. During the first step (incubation period), the contact angle decreases very slowly probably because of surface oxides and reaches 120° after about 140 min. In a second step, the drop starts spreading over the surface rapidly and penetrates the specimen. The contact angle decreases at a much higher rate and reaches 5° after 180 min.

For the S2-AS specimen, the shape of the curve in the second step is similar to that of the polished specimen for the same range of wetting angles. This suggests that the polishing eliminates surface oxides and impurities and reduces significantly the incubation period.

3.2. Early stage of interaction

To study step one and the early stage of the interaction between liquid aluminum and the as-sintered specimen, an experiment was carried out in which the test was interrupted after 100 min (specimen S3-PP). Fig. 3 shows the backscattered electron (BSE) micrograph from the cross section of the specimen-aluminum interface revealing the penetration of Al inside the specimen.

To investigate if counter-diffusion of elements from the TiB_2 specimen towards liquid Al is taken place, the cross section of the aluminum drop on top of the substrate was analyzed. Fig. 4(a) shows small white particles found inside the Al matrix. Semi-quantitative EDX analysis revealed that the composition of these particles corresponds to $TiAl_3$ phase. Particles of $TiAl_3$ are usually found in aluminum either as a needle-like structure or in the form of chunky equiaxed particles.[19] These results suggest that the Ti additives in TiB_2 dissolve and diffuse in the Al droplet during the test and precipitate as small $TiAl_3$ particles during solidification.[20–23]

Chemical mapping was performed in selected areas within the Al matrix. A Fe map is shown in Fig. 4(b). Contrary to Ti, which was mostly found in the form of Ti–Al particles, iron precipitated at grain boundaries during solidification.

These results indicate that the metallic Ti and Fe additives are dissolved in the liquid Al during the sessile drop tests and precipitate in the form of Ti and Fe aluminum phases upon solidification.

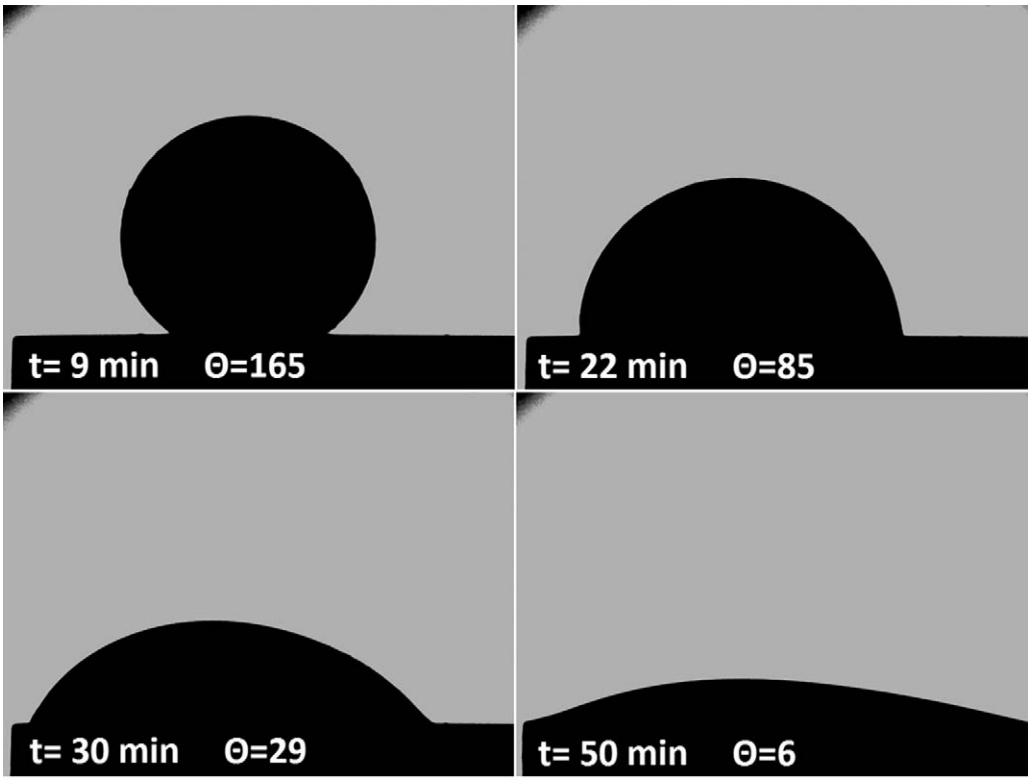

Fig. 1. Photos from the contact between a liquid Al drop and a polished specimen's surface during a sessile drop test.

The interface region between the Al droplet and the S3-PP specimen's surface was also analyzed using EPMA. Fig. 5(a) and (b) show the elemental distribution of aluminum and oxygen respectively in this region. The mapping of oxygen indicates a 20 μm thick oxide-rich layer near the interface. Comparison of this map with that of Al reveals that oxygen is present in the form of aluminum oxide. In the as-prepared specimen, oxygen is most likely picked-up by the Ti additives during the sintering process. During the sessile drop test, liquid Al reduces the Ti oxides to form aluminum oxide. A similar observation was also reported by Pettersen[13] when hot pressed TiB_2 specimens containing Ti additives were put in contact with liquid aluminum. Ti reacts with the oxygen present on the surface of TiB_2 particles and with the oxygen from the atmosphere to form trigonal Ti_2O_3 predominantly. He also mentioned that the reduction of this titanium oxide with liquid aluminum is thermodynamically feasible at temperatures around 1000 °C. According to our results, titanium oxide is present on the free surface of the particles and in the porosities. The reaction of titanium oxide with liquid aluminum may result in some reaction products with higher molar volume. However, the presence of about 9% of porosity in the specimen provides enough space for these volume changes and

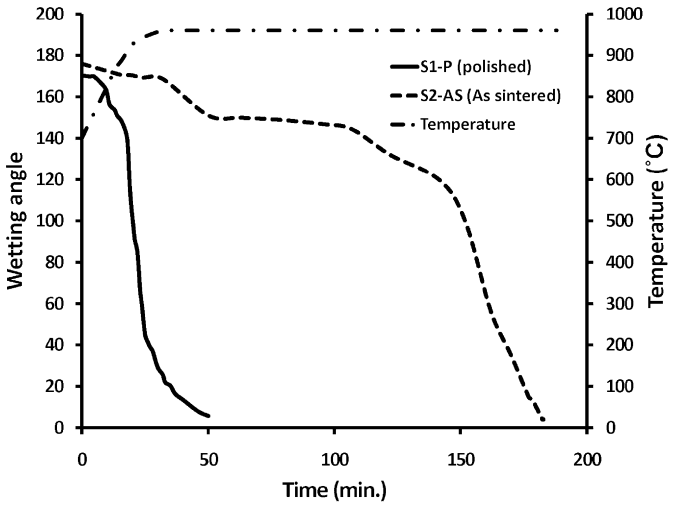

Fig. 2. Average contact angle versus time during sessile drop tests for the as-sintered and polished specimens.

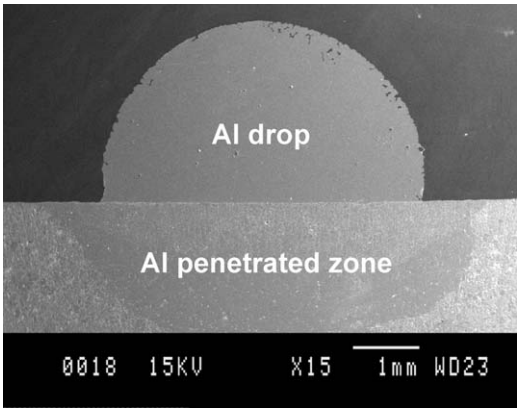

Fig. 3. BSE micrograph from the cross section of a specimen with partial penetration of Al (S3-PP).

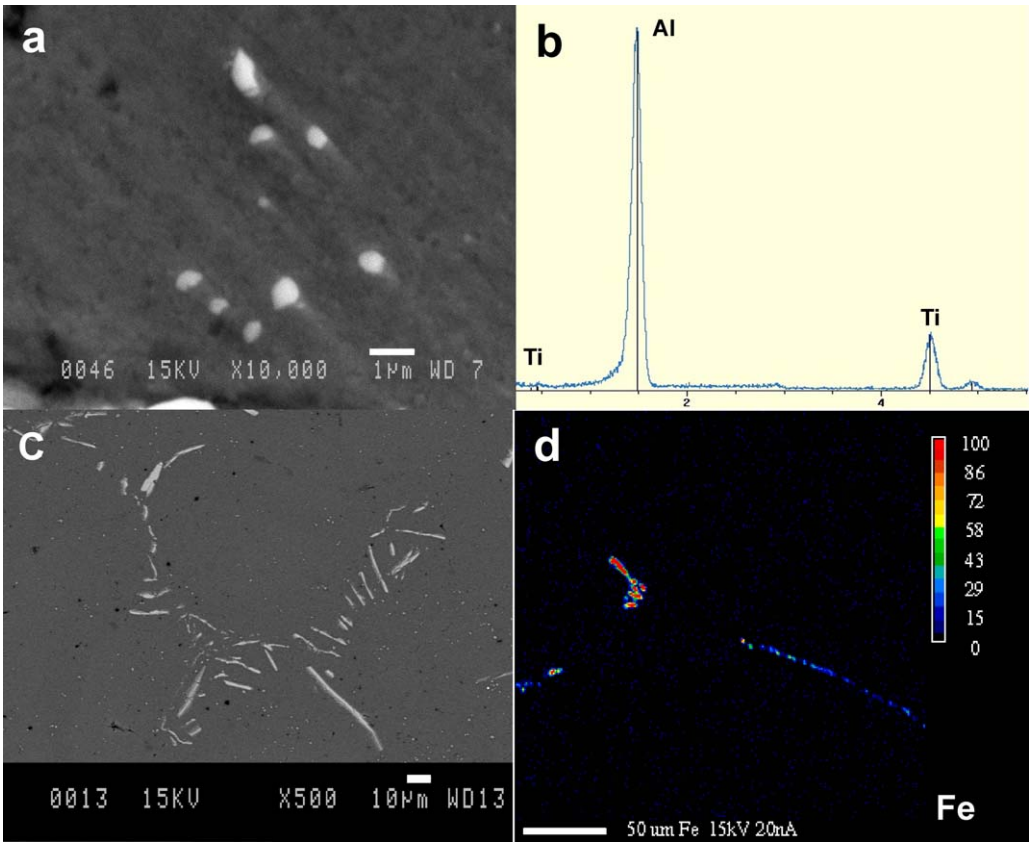

Fig. 4. Partially penetrated test (S3-PP) (a,b) BSE micrograph and EDX analysis of $TiAl_3$ particles formed inside Al drop, (c,d) BSE micrograph and EPMA maps of Fe element within Al drop.

thereby prevents the detachment of TiB_2 grains and specimen swelling.

The delay observed before the wetting takes place in the S2-AS case (Fig. 2) can therefore be explained by the presence of a thin oxide layer on the surface of sintered TiB_2. However, this surface oxide did not prevent full wetting of specimen ultimately.

3.3. Later stage of interaction

By examining the cross section of specimens after complete sessile drop test, it was found that the Al penetration resulted in the formation of four different zones. These zones are identified as zones 1–4 in Fig. 6. The zone 1 showed a high level of porosity with almost no sign of metallic additives. In zone 2 and zone 3, the pores contain Ti and Fe aluminum phases in addition of Al. These zones will be discussed in more details later in this work. Zone 4 remained intact. It represents the microstructure of the specimen before the sessile drop test.

Fig. 7 shows elemental line scans of Ti, Fe and Al through the cross section of the S1-P specimen. The approximate boundaries between the different zones are indicated by dotted-lines. The concentration of aluminum in zone 1 and 2 varies from point

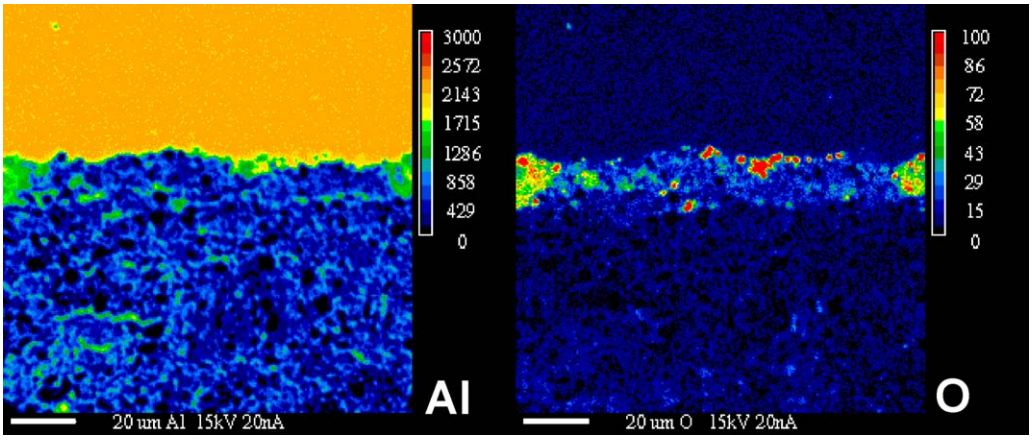

Fig. 5. Elemental distribution of aluminum and oxygen at the drop-specimen interface after the partially penetrated test (S3-PP).

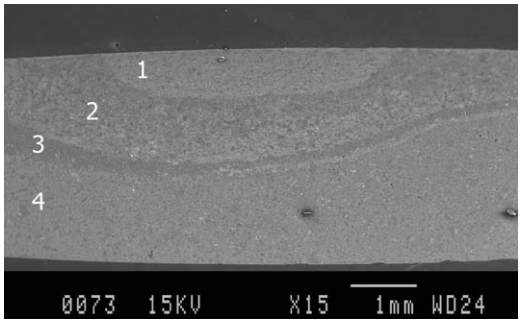

Fig. 6. SEM micrograph of the cross section of a S1-P specimen after the sessile drop test.

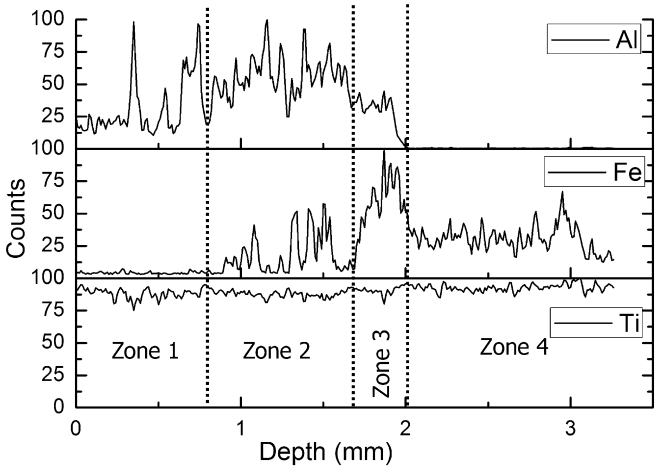

Fig. 7. Elemental line scans carried out through the thickness of the specimen after a sessile drop test at 960 °C. (Depth = 0 is corresponds to the aluminum-specimen interface at the beginning of the test).

to point depending on pore location and density. Its average concentration in zone 2 is considerably higher than that in zone 1. It seems that the Al concentration decreases in zone 3 and falls to zero in zone 4. There is a very low concentration of Fe in zone 1. Fe was detected at some points in zone 2 and its concentration increases and reaches a maximum in zone 3 before falling to the bulk Fe additive concentration of 3 wt% in zone 4. The Ti distribution in Fig. 7 shows only small variations since the signal comes from both TiB_2 particles and the Ti metallic additives.

Fig. 8 shows elemental maps of Ti and Al near the interface between zone 1 and 2. The maps seem to indicate that the Ti concentration in the pores where Al is present is lower in zone 1 (darker blue) than in zone 2 suggesting that the Ti additives have been washed out from zone 1 during the liquid infiltration. The simultaneous presence of Ti and Al in the pores of zone 2 suggests the presence of Ti–Al phases in this zone.

Fig. 9 shows the mapping of Fe and Ti near the interface of zones 2 and 3. The concentration of Fe in zone 3 is much higher than in zone 2 in agreement with Fig. 7. The Ti concentration in pores is lower (darker blue) in zone 3 than in zone 2 and in these pores, Fe is present instead of Ti. The simultaneous presence of Fe and Al in the pores of zone 3 suggests the presence of Fe–Al phases in zone 3.

Finally, Fig. 10 shows elemental maps near the transition between zones 3 and 4. The Al concentration decreases down to zero from zone 3 to zone 4 in agreement with the line scan of Fig. 7. The Ti content between the TiB_2 grains or in the pores seems to increase as we move from zone 3 to zone 4 in agreement with what as been said previously regarding zone 3.

Fig. 11(a) and (b) shows SEM images of the specimen in zone 2 and 3 respectively. In zone 2, the phase identified as P1 contains Ti and Al. Studies on the Ti–Al system have shown that at temperatures between 700 and 1000 °C, $TiAl_3$ is formed prior to any other titanium aluminide phases. It was also reported that this intermetallic compound can dissolve 1.2 at.% Fe at 1000 °C.[24] To verify the exact nature of this phase, TEM analysis was performed. A TEM micrograph of such a phase is shown in

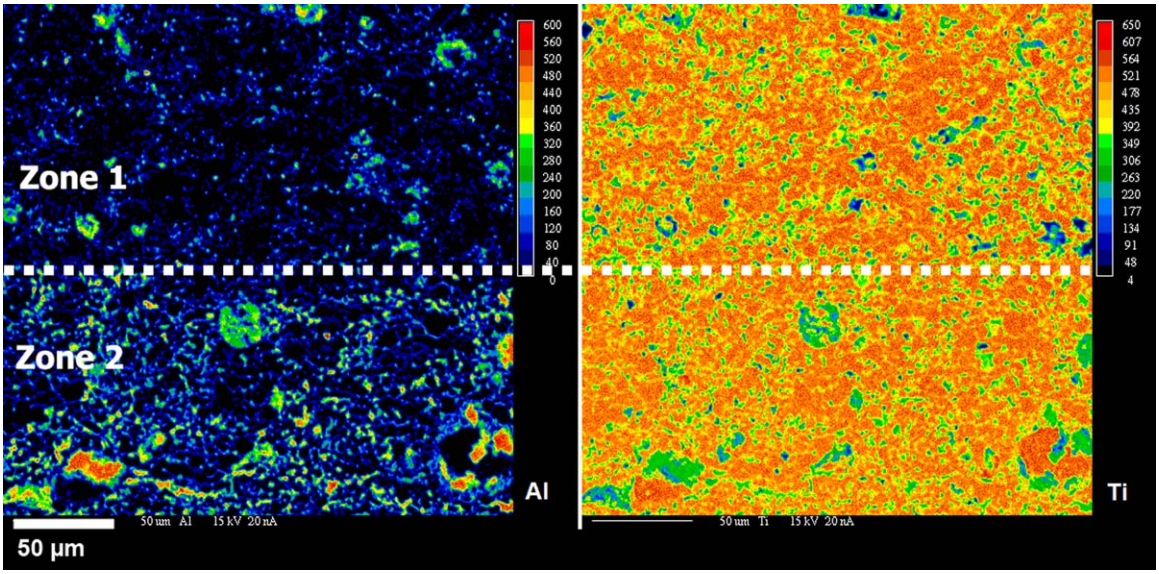

Fig. 8. Mapping of aluminum and titanium showing the transition between zone 1 and zone 2. (For interpretation of the references to color in text, the reader is referred to the web version of this article.)

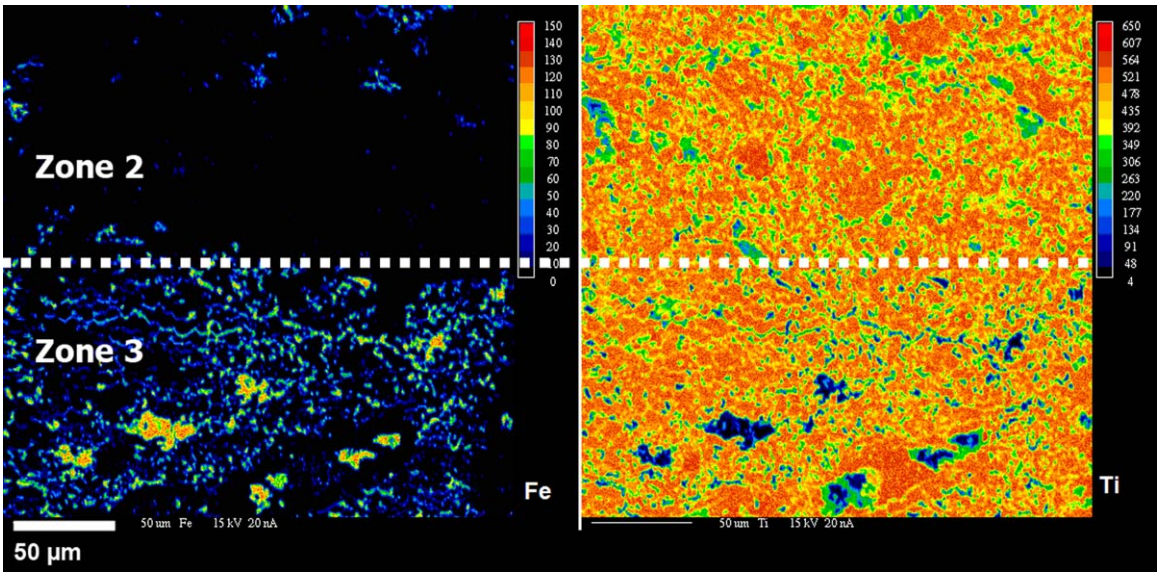

Fig. 9. Mapping of iron and titanium revealing the transition between zone 2 and zone 3. (For interpretation of the references to color in text, the reader is referred to the web version of this article.)

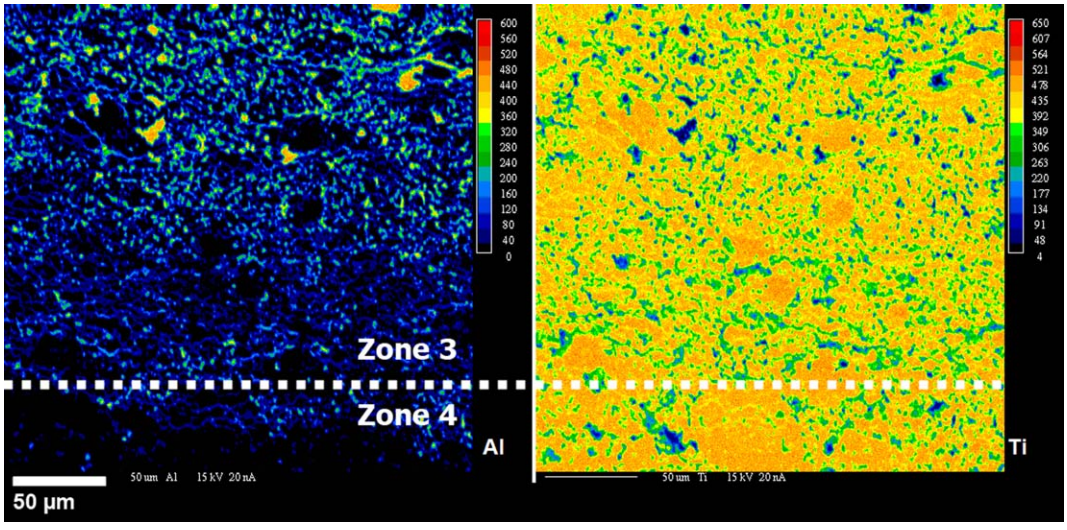

Fig. 10. Mapping of aluminum and titanium between zone 3 and zone 4.

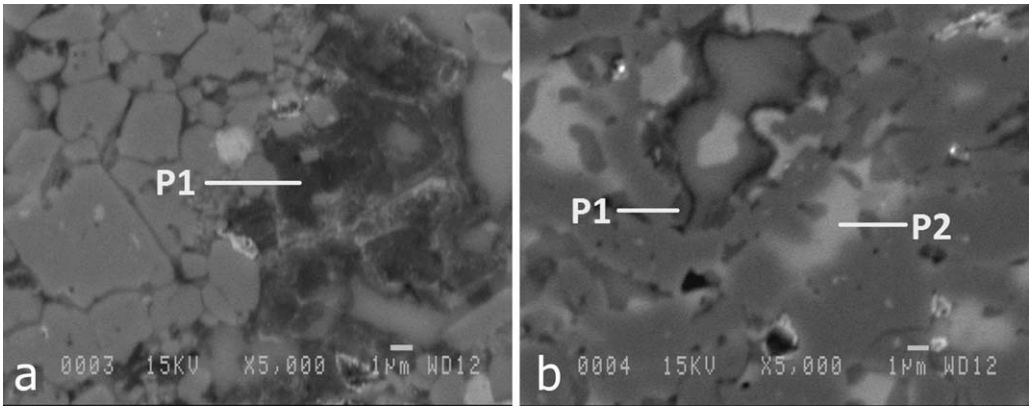

Fig. 11. BSE micrographs of zone 2 and zone 3. Arrows show the presence of $TiAl_3$ (P1) and Fe–Al compound (P2).

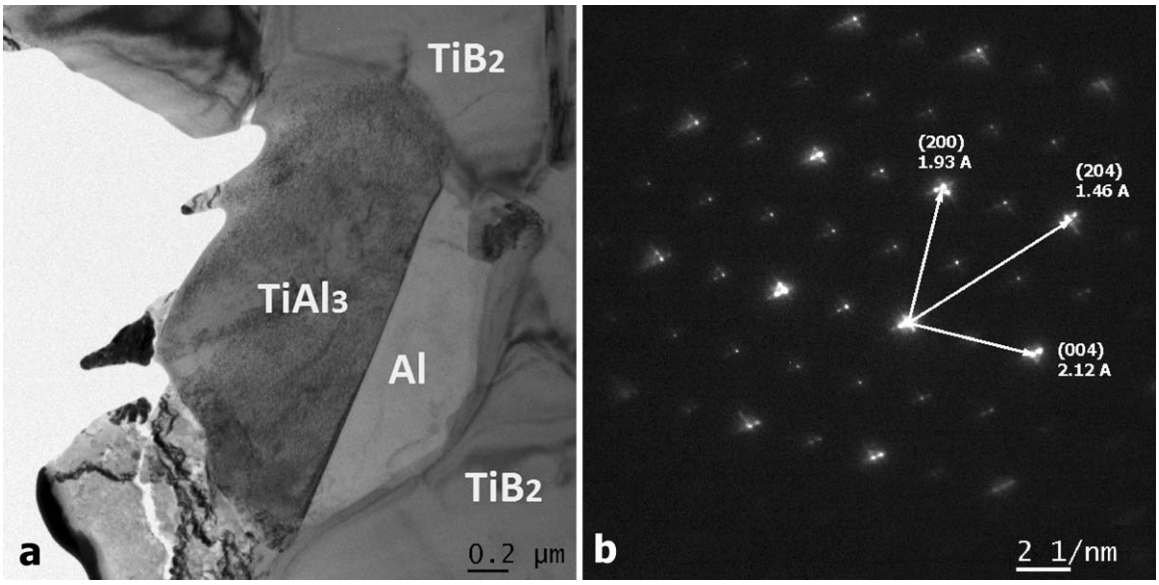

Fig. 12. $TiAl_3$ precipitate in zone 2, (a) Transmission electron micrograph, (b) SAED pattern from the [0 1 0] zone axis of $TiAl_3$.

Fig. 12(a). EDX analysis and the SAED pattern (Fig. 12(b)) taken from the [0 1 0] zone axis of P1 confirm that this phase is $TiAl_3$. This titanium aluminide phase precipitates from Ti saturated liquid Al in the pores between the TiB_2 particles when the liquid phase enters zone 2.

The phase identified as P2 in zone 3 (see Fig. 11(b)) contains Al and Fe with traces of Ti. The phase P1 is also detected in zone 3. Studies have shown that Fe_4Al_{13} and Fe_2Al_5 phases are more likely to precipitate in the Al rich side of the phase diagram.[25] Although the growth rate of Fe_2Al_5 is higher, the formation of Fe_4Al_{13} is dominant in Al-rich interfaces. Therefore, it is highly probable that the P2 phase is Fe_4Al_{13}. The Ti solid solubility limit in that phase is 6.5 at.%. Ti can partially replace Fe in certain crystallographic sites.[26,27]

TEM analysis was also performed on P2 observed in zone 3 to confirm the nature of the Fe_4Al_{13} phase (see Fig. 13(a) and (b)). The SAED pattern shown in Fig. 13(b) is characteristic of the Fe_4Al_{13} structure.

3.4. Reaction mechanism

Based on these results, the reaction mechanism between the liquid Al drop and the specimen could be described as follows. When liquid aluminum forms over the polished surface of the specimen, it interacts with surface oxides and three other major microstructural features: TiB_2 particles, pores, and the metallic additives. After the reduction of surface oxides by liquid aluminum and wetting of the TiB_2 particles, the metallic additives are dissolved and the liquid enters the pores. At the beginning of the test, the liquid is pure aluminum. As it enters the porous structure, the concentration of Ti and Fe in the liquid gradually increases. The liquid has a solubility limit for Fe and Ti above

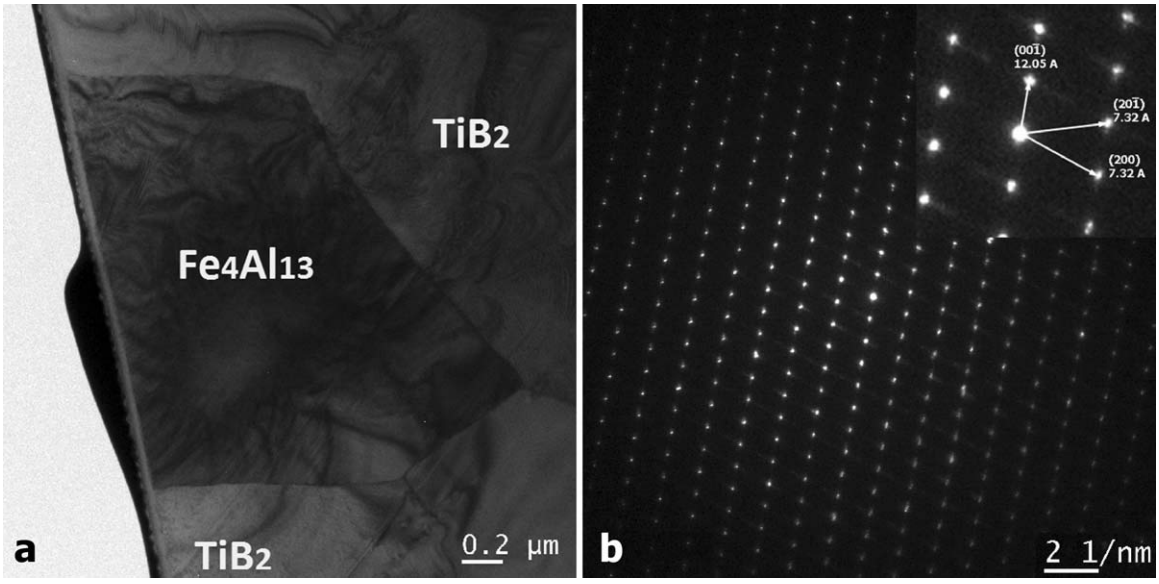

Fig. 13. Fe_4Al_{13} phase precipitated in zone 3, (a) Transmission electron micrograph, (b) SAED pattern from the [010] zone axis of Fe_4Al_{13}.

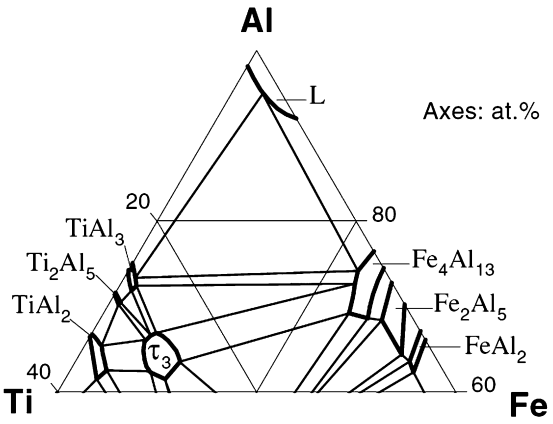

Fig. 14. Isothermal section of the Al–Fe–Ti phase diagram at 1000 °C.[20]

which new phases will precipitate. Based on the binary phase diagrams of Al–Fe and Al–Ti, the solubility limit of Fe and Ti in liquid aluminum at 960 °C is about 17 and 2 wt%, respectively. Fig. 14 shows the ternary phase diagram of Al–Ti–Fe. In this work, the Ti to Fe weight ratio was 7/3 and therefore, the concentration of Ti in the liquid should increase more rapidly than that of Fe.

Since the Fe and Ti content in the liquid is below the solubility limit in zone 1, the additives in this zone are simply dissolved while the aluminum is penetrating into the specimen. Once the concentration of Ti reaches the solubility limit near 2 wt%, $TiAl_3$ phase starts to precipitate forming zone 2. In this zone, the concentration of Fe is still below its solubility limit (17 wt%), thus Al continues to dissolve the additives and penetrates inside the specimen until the solubility limit of Fe is reached. This marks the beginning of zone 3 where the Fe_4Al_{13} phase is formed. At this point, the $TiAl_3$ phase continues to precipitate and this explains the presence of both P1 and P2 phases in zone 3. By the precipitation of Fe_4Al_{13} and $TiAl_3$, the liquid aluminum is gradually consumed. In the final stage of the reaction, the liquid aluminum acts as a "transient liquid phase"[28] which means that after the diffusion of iron and titanium in the remaining liquid, its transforms gradually to solid phases via isothermal solidification processes.

The formation of zone 3 where the liquid isothermally solidifies by the formation of aluminide phases raises the question on whether this zone could act as a barrier against further aluminum penetration. This hypothesis was put to test by performing an additional sessile drop test on the specimen formerly subjected to this test. The cross section micrograph of S4-2D specimen is shown in Fig. 15. Comparing the cross section of S4-2D with that of the S1-P specimen, we see that the penetration of the second aluminum drop lead to an increase of the width of zone 1, zone 2, and zone 3.

This observation suggests that the second drop follows the same reaction mechanism as the first one resulting in the dissolution of solid phases and precipitation of new phases until the solubility limits of Fe and Ti are reached. Zone 3 cannot act as a barrier to the penetration of liquid aluminum.

However, it is important to note that the TiB_2 specimens remained intact despite the penetration of liquid aluminum and

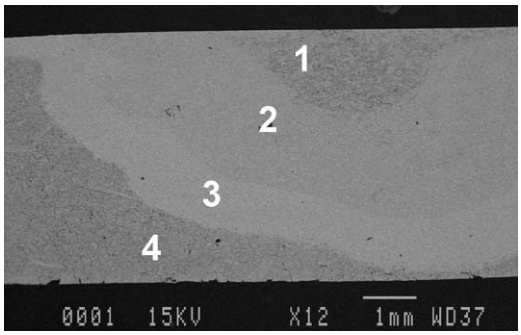

Fig. 15. SEM micrograph of cross section of specimen subjected to two subsequent sessile drop tests.

the dissolution of the metallic additives. This could be attributed to the stability of the grain boundaries (bridges) between the TiB_2 particles. The boundaries formed between the TiB_2 particles during sintering with Ti–Fe additives are quite stable in liquid Al. The specimens did not show any swelling or crack in the microstructure. The expansion of the structure of TiB_2 sintered using transitional methods has already been reported in the literature.[29] Further investigations concerning the stability of these TiB_2 composites in liquid Al will be presented in an upcoming publication.

4. Conclusion

The interaction of TiB_2-base porous ceramics with liquid Al was investigated. The reactions were occurring faster on polished surfaces because of the removal of the surface oxide layer. The penetration of the liquid Al drop resulted in the formation of three distinct zones. Only Al was found in the first zone, $TiAl_3$ was found in the second zone and both $TiAl_3$ and Fe_4Al_{13} phases were found in the third zone. When penetration of liquid Al into the material occurs, the metallic additives are dissolved and their concentration increases gradually. Once the Ti saturation limit is achieved, the $TiAl_3$ phase starts to precipitate inside the pores (zone 2). The residual liquid continues to penetrate and dissolve the additives until the saturation point of Fe is reached leading to the precipitation of Fe_4Al_{13} (zone 3). Dissolution and precipitation will continue up to the complete depletion of the liquid phase (Isothermal solidification). Liquid aluminum did not seem to alter the solid TiB_2 skeleton of the specimen and no sign of swelling or cracking was detected.

Acknowledgements

The authors wish to acknowledge the kind contribution of the technicians of the Dept. of Mining, Metallurgical and Materials Engineering of Laval University, of Sylvio Savoie from Hydro-Quebec and of Jean-Philippe Masse from École Polytechnique de Montréal for TEM analysis. The financial support of this project was provided by Hydro Quebec and the Natural Sciences and Engineering Research Council of Canada (NSERC). The research project was also partially financed by the "Fonds Québécois de la Recherche sur la Nature et les Technologies (FQRNT)" via the Aluminum Research Centre–REGAL.

References

1. Hatch JE. *Aluminum: properties and physical metallurgy*. Metals Park, OH: American Society for Metals; 1984.
2. Sørlie M, Øye HA. Inert and wettable cathodes. In: *Cathodes in aluminium electrolysis.* Düsseldorf: Aluminium-Verlag; 1994. pp. 66–70.
3. Billehaug K, Øye HA. Inert cathodes for aluminum electrolysis in Hall–Heroult cells. Pt. I. *Aluminum* 1980;**56**:642–8.
4. Richerson DW. Aluminum industry. In: Freitag DW, Richerson DW, editors. *Opportunities for advanced ceramics to meet the needs of the industries of the future*. US Office of Energy; 1998.
5. Basu B, Raju GB, Suri AK. Processing and properties of monolithic TiB_2 based materials. *Int Mater Rev* 2006;**51**:352–74.
6. Cutler RA. Engineering properties of borides. In: Schneider SJ, editor. *Engineering materials handbook, ceramic and glasses*. Metals Park, OH, USA: ASM International; 1991. p. 787–803.
7. Barandika MG, Echeberría JJ, Sánchez JM, Castro F. Consolidation, microstructure, and mechanical properties of a TiB_2–Ni_3Al composite. *Mater Res Bull* 1999;**34**:53–61.
8. Baik S, Becher PF. Effect of oxygen contamination on densification of TiB_2. *J Am Ceram Soc* 1987;**70**:527–30.
9. McMinn CJ. Review of RHM cathode development. In: *Light Metals 1992.*; 1992. pp. 419–425.
10. Dorward RC. Aluminum penetration and fracture of titanium diboride. *J Am Ceram Soc* 1982;**65**:C-6.
11. Jensen MS, Pezzotta M, Zhang ZL, Einarsrud MA, Grande T. Degradation of TiB_2 ceramics in liquid aluminum. *J Eur Ceram Soc* 2008;**28**: 3155–64.
12. Kang SH, Kim DJ, Kang ES, Baek SS. Pressureless sintering and properties of titanium diboride ceramics containing chromium and iron. *J Am Ceram Soc* 2001;**84**:893–5.
13. Pettersen G. *Development of microstructure during sintering and aluminium exposure of titanium diboride ceramics*. Norway: Department of Physics, NTNU; 1997. p. 138.
14. Einarsrud M-A, Hagen E, Pettersen G, Grande T. Pressureless sintering of titanium diboride with nickel, nickel boride, and iron additives. *J Am Ceram Soc* 1997;**80**:3013–20.
15. Heidari H, Alamdari H, Dubé D, Schulz R. Pressureless sintering of TiB_2-based composites using Ti and Fe additives for development of wettable cathodes. In: *Light Metals 2011.*; 2011. pp. 1111–1116.
16. Heidari H, Alamdari H, Dubé D, Schulz R. Investigating the potential of TiB2-based composites with Ti and Fe additives as wettable cathode. Mater Sci Forum; in press.
17. Nord-Varhaug K. TEM investigation of impurity phases and the penetration of liquid aluminum in hot isostatically pressed TiB_2 compacts. *J Am Ceram Soc* 1996;**79**:1147–54.
18. Rhee SK. Wetting of ceramics by liquid aluminum. *J Am Ceram Soc* 1970;**53**:386–9.
19. Jones G, Pearson J. Factors affecting the grain-refinement of aluminum using titanium and boron additives. *Metall Mater Trans B* 1976;**7**:223–34.
20. Ghosh G. Al–Fe–Ti (Aluminium–Iron–Titanium). In: Effenberg G, Ilyenko S, editors. *Light metal ternary systems: phase diagrams, crystallographic and thermodynamic data*. 2005.
21. Kattner U, Lin J, Chang Y. Thermodynamic assessment and calculation of the Ti–Al system. *Metall Mater Trans A* 1992;**23**:2081–90.
22. Palm M, Lacaze J. Assessment of the Al–Fe–Ti system. *Intermetallics* 2005;**14**:1291–303.
23. Raghavan V. Al–Fe–Ti (aluminum–iron–titanium). *J Phase Equilib* 2002;**23**:367–74.
24. Palm M, Inden G, Thomas N. The Fe–Al–Ti system. *J Phase Equilib* 1995;**16**:209–22.
25. Shahverdi HR, Ghomashchi MR, Shabestari S, Hejazi J. Microstructural analysis of interfacial reaction between molten aluminium and solid iron. *J Mater Process Tech* 2002;**124**:345–52.
26. Grin J, Burkhardt U, Ellner M, Peters K. Refinement of the Fe_4Al_{13} structure and its relationship to the quasihomological homeotypical structures. *Z Krist-New Cryst St* 1994;**209**:479–87.
27. Yanson TI, Manyako NB, Bodak OI, Cêrny R, Gladyshevskii RE, Yvon K. Crystal structure of $Fe_4Ti_{0.93}Al_{12.07}$, a substitutional variant of the Fe_4Al_{13} structure type. *J Alloys Compd* 1995;**219**:135–8.
28. MacDonald WD, Eagar TW. Transient liquid phase bonding. *Annu Rev Mater Sci* 1992;**22**:23–46.
29. Weirauch D, Krafick W, Ackart G, Ownby P. The wettability of titanium diboride by molten aluminum drops. *J Mater Sci* 2005;**40**:2301–6.